

Source Camera Verification for Strongly Stabilized Videos

Enes Altinisik, Hüsrev Taha Sencar

Abstract—The in-camera image stabilization technology deployed by most cameras today poses one of the most significant challenges to photo-response non-uniformity based source camera attribution from videos. When performed digitally, stabilization involves cropping, warping, and inpainting of video frames to eliminate unwanted camera motion. Hence, successful attribution requires inversion of these transformations in a blind manner. To address this challenge, we introduce a source camera verification method for videos that takes into account spatially variant nature of stabilization transformations and assumes a larger degree of freedom in their search. Our method identifies transformations at a sub-frame level and incorporates a number of constraints to validate their correctness. The method also adopts a holistic approach in countering disruptive effects of other video generation steps, such as video coding and downsizing, for more reliable attribution. Tests performed on one public and two custom datasets show that proposed method is able to verify the source of 23-40% of videos that underwent stronger stabilization without a significant impact on false attribution rate.

I. INTRODUCTION

Photo-response non-uniformity (PRNU) is an intrinsic characteristic of a digital imaging sensor that reveals itself as a unique and permanent pattern introduced to all media captured by the sensor. The PRNU of a sensor is proven to be a viable identifier for source attribution, and it has been successfully utilized for identification and verification of the source of digital media. In the past decade, various approaches have been proposed for reliable estimation, compact representation, and faster matching of PRNU patterns. These studies, however, mainly featured photographic images, and videos have been largely neglected. In essence, steps involved in generation of a video are much more disruptive to PRNU pattern, and therefore its estimation from videos involves various additional challenges.

PRNU is caused by variations in size and material properties among photosensitive elements that comprise a sensor. These essentially affect the response of each picture element under the same amount of illumination. Therefore the process of identification boils down to quantifying the sensitivity of each picture element. This is realized through an estimation procedure using a set of pictures acquired by the sensor [1]. To determine whether a media is captured by a given sensor, the estimated sensitivity profile, *i.e.*, the PRNU pattern, from the media in question is compared to a reference PRNU pattern obtained in advance using a correlation based measure, most typically using the peak-to-correlation energy (PCE) [2]. The reliability and accuracy of the decision strongly depend on two main factors. First relates to the fact that the PRNU bearing raw signal at the sensor output has to pass through several steps of in-camera processing before a media is generated, which

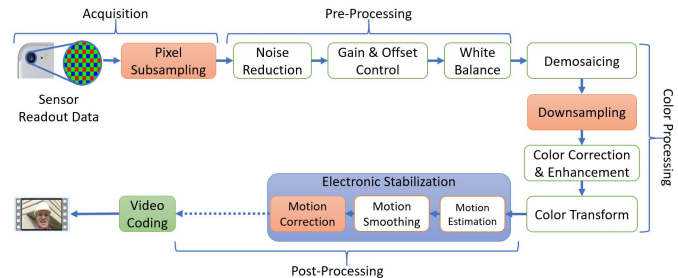


Fig. 1. The processing steps involved in the imaging pipeline of camera when generating a video. The highlighted boxes are specific to video capture.

may further be subjected to some out-of-camera processing. These processing steps will have a weakening effect on the inherent PRNU pattern. Second, and more critically, it relies on preserving the element-wise correspondences between the reference pattern and the PRNU pattern estimated from the media in question.

The imaging sub-systems used by digital cameras largely remain proprietary to the manufacturer; therefore, it is quite difficult to access their details. At a higher level, however, the imaging pipeline in a camera includes various stages, such as acquisition, pre-processing, color-processing, post-processing, and image and video coding. Figure 1 shows basic processing steps involved in capturing a video, most of which are also utilized during the acquisition of a photograph [3]. When generating a video, an indispensable processing step is the downsizing of the full-frame sensor output to reduce the amount of data that needs processing. This may be realized at acquisition by subsampling pixel readout data (through binning [4] or skipping [5] pixels), as well as during color processing by downsampling color interpolated image data. Another key processing step employed by modern day cameras at post-processing stage is the electronic image stabilization which aims at compensating camera shake related blur. It must be noted that even such post-processing may include operations, such as cropping and scaling, that result with further downsizing of pictures. At last, the sequence of post-processed pictures are encoded into a standard video format for effective storage and transfer.

Crucially, video generation involves three additional steps as compared to the generation of photos, including downsizing, stabilization, and video coding. When combined together, these operations have a significant adverse impact on PRNU estimation in two main respects. These relate to geometric transformations applied during downsizing and stabilization and the information loss largely caused by resolution reduction and compression. Therefore, estimation of a sensor's PRNU

from videos requires addressing these challenges.

A number of approaches have already been proposed to address these problems with different degrees of effectiveness. Earlier works mostly focused on coping with compression as it is typically more lossy for videos than images. To obtain a better PRNU estimate, Chen *et al.* [6] considered removal of periodic structures in the PRNU pattern that arise due to block-based operation of encoder; Hyun *et al.* [7] introduced the use of minimum average correlation energy filter to better suppress compression related noise during matching; and Chuang *et al.* [8], observing intracoded (I) frames yield more reliable PRNU patterns than predicted (P and B) frames, suggested weighting I frames more heavily during estimation. More recently introduced approaches proactively intervene in the decoding process to compensate for the deblocking filter [9] and incorporate macroblock level compression information into estimation process [10].

The weakening of effect of downscaling on PRNU pattern was long observed. In [11], it is shown that downsizing high-resolution sensor output by a factor higher than six removes almost all traces of PRNU pattern in a video, even for very high quality videos, when the specifics of downsizing method are not known. Moreover, downsizing is also a concern because of the geometric distortions it introduces on the PRNU pattern as cameras can capture media at a variety of resolutions. Therefore, mismatches in resolution between a reference PRNU pattern and a media need to be taken into consideration. References [11], [12], and [13] examined in-camera downsizing behavior to enable reliable matching of PRNU patterns at different resolutions.

In regards to preserving synchronicity between PRNU patterns, the most significant challenge is posed by image stabilization. When performed electronically, stabilization requires estimating and removing undesired camera motion due to handheld shooting or other vibrations. This involves the application of geometric transformations to align successive frames in a video with respect to each other. From the PRNU estimation standpoint, this requires registration of PRNU patterns by inverting transformations applied to each frame in a blind manner. Ultimately, the difficulty of this task depends on the type of stabilization transformations applied to video frames. For the sake of clarity, in this work, we refer to videos that can be attributed through application of frame-level affine transformations as *weakly stabilized* videos and those that require more complicated transformation inversion settings as *strongly stabilized* videos.

The approaches proposed so far to deal with stabilization focused on a variety of aspects including determining the presence of stabilization in video [14] as well as verifying the source of a video by evaluating frame-level matches [12] and obtaining a reference PRNU from weakly stabilized videos [15] under an affine transformation model. Our main contribution in this work lies in extending source verification capability, which assumes the presence of camera’s reference PRNU pattern, to strongly stabilized videos. Essentially, inspired by the approach introduced in [16], many proposed stabilization methods effectively involve application of spatially varying warps during stabilization. By taking this into account, our

work departs from earlier attribution approaches in its premise that stabilization transformations may exhibit locality and not necessarily be applied at the frame level as assumed by prior work.

More specifically, our proposed method for verifying source of stabilized videos differs from earlier methods in two main aspects. First, in countering the variant nature of stabilization transformations, our method operates on blocks of frames, rather than on individual frames. To avoid blocks whose content partially underwent multiple warpings, we evaluate the coherence of matching results obtained at the block and sub-block levels. Second, in reverting the transformation applied to each block, we consider projective transformations, as opposed to affine transformations, which provide wider flexibility in identifying the unwanted motion removed by the stabilization. Our approach also incorporates findings on mitigation of video compression effects [10] and downsizing behavior [11] to develop a holistic solution. The proposed method is validated on three datasets. These include the publicly available VISION dataset [17] and two custom datasets¹. One of the newly generated datasets include media captured by two iPhone camera models (the iPhone SE-XR dataset) and the other includes a set of externally stabilized videos using the Adobe Premiere Pro video processing tool (the APS dataset). To evaluate the true potential of the method, tests are performed on subset of videos obtained after excluding all weakly stabilized videos identified using existing approaches. Results show that proposed method is able to correctly attribute 23-40% of strongly stabilized videos, with an overall correct attribution rate of 30%, without any false-positive attributions while utilizing only 5-10 frames.

In the next section, we describe how image stabilization is performed and provide an overview of proposed approaches for source attribution on stabilized videos. In section III, we address challenges in attributing stabilized videos with excessive camera motion. Details of our method are described in Section IV and performance results are presented in the V. Finally, our discussion on the results is given in Section VI.

II. VIDEO STABILIZATION

With the increasing processing power built into cameras and the advances in lens technologies, increasingly more powerful stabilization solutions have become available on cameras. There are two primary approaches to image stabilization. The first one is the optical stabilization. In this approach, stabilization is performed mechanically through the use of hardware based mechanisms, and the movement of the camera is not fully transferred to the video. Rather, it is absorbed by moving the lens or the imaging sensor to counter the unwanted motion. Since optical stabilization preserves pixel-to-pixel correspondences in successive frames, it does not obstruct PRNU based source attribution.

The other approach is the digital stabilization where frames captured by the sensor are moved and warped to align with one

¹The two newly generated datasets and the implementation for the proposed approach can be obtained at <https://github.com/VideoPRNUExtractor> following final modifications, prior to publication of this manuscript.

another through processing. With this approach, the movement of the camera is estimated either from sequence of frames or using available sensors on the device. Then, corrective stabilization transforms associated with the estimated motion are determined, and each frame is transformed and saved accordingly. This frame level processing introduces an asynchronicity among PRNU patterns of consecutive frames in a video which can be detrimental to PRNU based source attribution.

Attribution of digitally stabilized videos requires understanding the specifics of how stabilization is performed. This, however, is a challenging task as inner workings and technical details of processing steps of camera pipelines are usually not revealed. In fact, both stabilization approaches can be deployed together in a camera for more effective results [18]. Further, even in the absence of abrupt camera motion the vibrations caused by physiological hand tremor may induce undesirable blur in videos [19]; therefore, when performed digitally, stabilization effects can potentially be present in most videos.

At a high level, the three main steps of digital stabilization involve camera motion estimation, motion smoothing, and alignment of video frames according to the corrected camera motion. Motion estimation is performed either by describing the geometric relation between consecutive frames through a parametric model or through tracking key feature points across frames to obtain feature trajectories [20], [21]. With sensor-rich devices such as smartphones and tablets becoming the primary camera, data from motion sensors are also utilized to improve the estimation accuracy [22]. This is followed by application of a smoothing operation to estimated camera motion or obtained feature trajectories to eliminate the unwanted motion. Finally, each frame is warped according to the smoothed motion parameters to generate the stabilized video.

The most critical factor in stabilization depends on whether the camera motion is represented by a two dimensional (2D) or three dimensional (3D) model. Early methods mainly relied on the 2D motion model that involves application of full-frame 2D transformations, such as affine or projective models, to each frame during stabilization. Although this motion model is effective in scenes far away from camera where parallax is not a concern, it does not generalize to more complicated scenes captured under spatially variant camera motion. To overcome 2D modelling limitations, more sophisticated methods considered 3D motion models. However, due to difficulties in 3D reconstruction, which requires depth information, these methods introduce simplifications to 3D structure and rely heavily on the accuracy of feature tracking [16], [23]–[25]. Most critically, these methods involve the application of spatially-variant warping to video frames in a way that preserves the content from distortions introduced by such local transformations. This poses a significant complication to PRNU based source attribution, as for each frame it requires determining the inverse warping parameters at a local level, and not globally.

To demonstrate the effect of stabilization on a video, we performed a test using the iMovie video editing tool that runs on Mac OS computers and iOS mobile devices. For this

purpose, we shot a video by panning the camera around a still indoors scene while stabilization and electronic zoom were turned off. The video is then stabilized by iMovie at 10% stabilization setting which determines the maximum amount of cropping that can be applied to each frame during alignment. To evaluate the nature of warping applied to video frames, we extracted Kanade–Lucas–Tomasi (KLT) reference feature points [26] that are frequently used to estimate the motion of keypoints [27]. Then, displacements of KLT points in pre- and post-stabilized video frames are measured. Figure 2 shows the optical flows estimated using KLT points for two sample frames. As can be seen, KLT points in a given locality move similarly, mostly inwards due to cropping and scaling. However, a single global transformation that will cover the movement of all points seems unlikely. In fact, our attempts to determine a single warp transformation to map key points in successive frames failed with only 4-5, out of the typical 50, points resulting with a match. Overall, this supports the intuition that digital image stabilization solutions available in today’s cameras are deploying sophisticated methods to smooth camera motion.

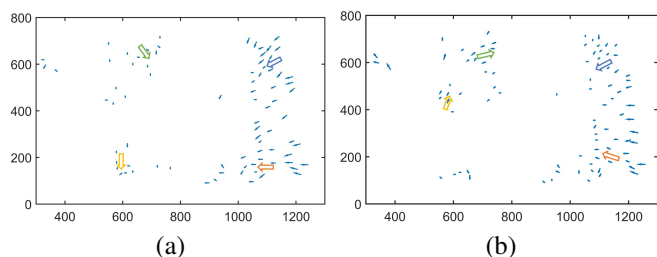


Fig. 2. KLT feature point displacements in two sample frames in a video stabilized using the iMovie editing tool at 0.1 stabilization setting. Displacements are measured in reference to stabilized frames.

A. Work on Attribution of Stabilized Videos

In essence, digital image stabilization tries to align content in successive frames through geometric registration. Depending on the complexity of camera motion during capture, this may include application of a simple Euclidean transformation (scale, rotation, and shift applied individually or in combination) to spatially-varying warping transformation in order to compensate for any type of perspective distortion. Because these transformations are applied on a per-frame basis and the variance of camera motion is high enough to easily remove pixel to pixel correspondences among frames, alignment or averaging of frame level PRNU patterns will not be very effective in estimating a reference PRNU pattern. Therefore, performing source attribution in stabilized video requires determining and inverting those transformations applied at the frame level.

Source attribution under geometric transformations was studied earlier to verify the source of transformed images when the reference PRNU pattern is available. Considering scaled and cropped photographic images, Goljan *et al.* [28] proposed a brute force search for the geometric transform parameters. For this, the PRNU pattern obtained from the image in question is upsampled in discrete steps and matched with the reference PRNU at all shifts. The parameters that yield the

highest PCE are identified as the correct scaling factor and the cropping position. More relevantly, by focusing on panoramic images, Karakucuk *et al.* [29] investigated source attribution under more complex geometric transformations. Their work showed the feasibility of estimating inverse transform parameters considering projective transformations.

In the case of stabilized videos, Taspinar *et al.* [14] proposed determining the presence of stabilization in a video by extracting reference PRNU patterns from the beginning and end of a video and by testing the match of the two patterns. If stabilization is detected, one of the I frames is designated as a reference and other I frames are aligned with respect to it through a search of inverse affine transforms to correct for the applied shift and rotation. The pattern obtained from the aligned I frames is then matched with a reference PRNU pattern obtained from a non-stabilized video by performing another search. The approach is validated on manually stabilized videos using FFMPEG deshaker.

Iuliani *et al.* [12] introduced another source verification method similar to [14] by additionally assuming the reference PRNU pattern might have been obtained from photos as well as from a non-stabilized video. That is, the video in question may have a different resolution than the reference PRNU pattern, and this mismatch in scales need to be taken into account during matching. To perform verification, 5-10 I frames are extracted and corresponding PRNU patterns are aligned with the reference PRNU pattern by searching for the correct amount of scale, shift and cropping applied to each frame. Those frames that yield a matching statistic above some predetermined PCE value are combined together to create an aligned PRNU pattern. Tests performed on videos captured by 8 cameras in the VISION dataset using first 5 frames of each video revealed that 86% of videos captured by cameras that support stabilization in the reduced dataset can be correctly attributed to their source with no false positives. They showed that the method is also effective on a subset of videos downloaded from YouTube with an overall accuracy of 87.3%.

In [15], Mandelli *et al.* introduced a method for estimating the PRNU pattern considering weakly stabilized videos. In this approach, a reference for alignment is generated from a set of frames. For this, PRNU estimates obtained from each frame is matched with other frames in a pair-wise manner to identify those translated with respect to each other. Then the largest group of frames that yield a sufficient match are combined together to obtain an interim reference PRNU pattern and remaining frames are aligned with respect to this pattern. Alternatively, if the the reference PRNU pattern at a different resolution is already known, then this is used a reference and PRNU patterns of all other frames are matched by searching for transform parameters using particle swarm optimization. They observed that for weakly stabilized videos, rotation can be ignored to speed up the search.

When performing source verification, sensor's PRNU pattern is first estimated from a weakly stabilized flat and still content videos as described above. For verification, five I frames extracted from the stabilized video are matched to this reference PRNU pattern considering a scaling by a factor of

0.99 to 1.01, rotations of -0.15 to 0.15 radians, and all possible shift positions. If the resulting PCE values for at least one of the frames is observed to be higher than a threshold, a match is assumed to be achieved. Results obtained on the VISION dataset show that the method is effective in successfully attributing 71% and 77% of videos captured by cameras that support stabilization with 1% false positive rate, respectively, when 5 and 10 I frames are used while excluding the first I frame as it is less likely to be stabilized. Alternatively, if the reference PRNU pattern is extracted from photos, rather than flat videos, under the same conditions attribution rates increase to 87% for 5 frames and to 91% for 10 frames.

We next describe other challenges involved in dealing with stabilized videos captured under more severe camera motion and introduce our approach that is complementary to above methods in dealing this subset of videos.

III. ADDITIONAL CHALLENGES

The difficulty of inverting per-frame warping transformations is further exacerbated by additional factors. Video frames have lower resolutions than the full-sensor resolution typically used for acquiring photos. Therefore, a reference PRNU pattern estimated from photos provides a more comprehensive characteristic, but its use for video source verification potentially introduces a mismatch with the size of video frames. Essentially, downsizing operation in a camera involves various proprietary hardware and software mechanisms that crucially involve sensor cropping and resizing. Performing source attribution on stabilized video requires determining such device dependent parameters in advance. When this is not possible, the search for inverse warping transformations has to incorporate the search for these parameters as well.

Lower PCE values observed in matching PRNU patterns obtained from videos, as compared to those from photos, yields another complication. This decrease in PCE values is primarily caused by downsizing operation and video compression. When the PRNU pattern is estimated from multiple video frames, downsizing can be ignored as a factor as long as the resizing factor is higher than $\frac{1}{6}$ and compression becomes the main concern [11]. As demonstrated in [10], at medium to low compression levels, average PCE values drop significantly as compression gets more severe. Accordingly, reference patterns extracted from 36 raw videos captured by 28 cameras that are downsized in-camera by a factor of four and compressed at 2 Mbps, 900 Kbps and 600 Kbps bit rates, respectively, yielded average PCE values of 2000, 300, and 40. Alternatively, when PRNU patterns from video frames are individually matched with the reference pattern (*i.e.*, frame-to-reference matching), even downsizing by a factor of 2 causes significant reduction in measured PCE values [30]. Tests performed on 14 videos captured by 7 cameras at a resolution of 1920×1080 pixels by performing frame-to-reference matching revealed that resulting PCE values are mostly around 20, and below 40 for almost all frames. This introduces a significant challenge in the search of the correct transformation parameters.

Another issue concerns the difficulty of setting a decision threshold for matching. Large scale tests performed on

photographic images show that setting the PCE value to 60 as a threshold yields extremely low false-matches when the correct-match rate is quite high. In contrast, as demonstrated in the results of earlier works, where decision thresholds of 40-100 [12] and 60 [15] are utilized when performing frame-to-reference matching, such threshold values on video frames yield much lower attribution rates.

Some of the in-camera processing steps introduce artefacts that obstruct correct attribution. The biases introduced to PRNU estimate by the demosaicing operation and blockiness caused by compression are known to introduce periodic structures onto the estimated PRNU pattern. These artefacts can essentially be treated as pilot signals to derive clues about the transformation history of media after the acquisition. In fact for the case of photos, the linear pattern associated with the demosaicing operation has shown to be effective in determining the amount of shift, rotation, and translation, with weaker presence in newer cameras [31]. In the case of videos, the linear-pattern is observed to be even weaker most likely due to application of in-camera downsizing and more aggressive compression of video frames as compared to photos. Therefore, it cannot be reliably utilized in identifying global or local transformations. In a similar manner, since video coding uses variable block sizes determined adaptively during encoding, blockiness artefact is also not useful in reducing the computational complexity of determining the warping transformation.

Finally, the first frame of a video can be thought to be less affected from stabilization as most motion smoothing methods correct motion with respect to a reference frame [32], which might be selected as the first frame. In [15], it is reported that the first frame of videos in the VISION dataset are mostly non-stabilized. Our measurements also verify that, assuming a translation motion model, the first frame in 209 of those 257 videos in the VISION dataset yields a PCE value higher than 60. However, this finding does not hold for any of the videos in the newly generated iPhone SE-XR dataset. Hence, for some cameras, it seems stabilization gets activated when the camera is set to video mode, even before recording starts; therefore, the first frame cannot be solely relied on as the basis of attribution.

IV. PROPOSED METHOD

Our approach to attribution of stabilized videos assumes a source verification setting where a given video is matched against a known camera. That is, the reference PRNU pattern is assumed to be available. Our method comprises seven main steps. First, the bitstream is decoded into video frames while compensating for the effects of a filtering procedure applied at the decoder (*i.e.*, the loop filter) to reduce coding artefacts. Then, a PRNU pattern is extracted from each extracted frame. Before the analysis, the video is also tested for the severity of stabilization to eliminate unstabilized and weakly stabilized videos which can be attributed by existing methods. This is followed by cropping out smaller blocks from each PRNU pattern to cope with spatially variant nature of stabilization transformations. A search is performed to identify

transformation parameters for each PRNU block along with a validation step to prevent incorrect inversions. The inverse-transformed blocks are then combined together by a weighting procedure that takes into account the compression level of each block. The estimated PRNU pattern is finally compared against the reference PRNU pattern to evaluate the match. Figure 3 presents the sequence of attribution steps.

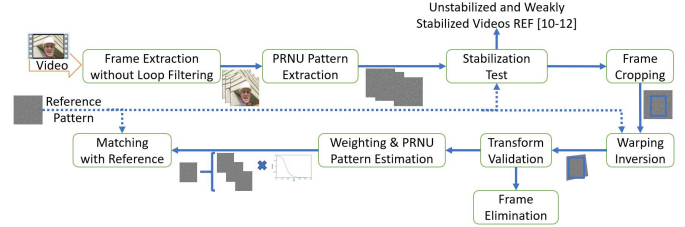


Fig. 3. Source camera verification steps for stabilized videos.

A. Loop filter compensation

Compression is the last step in video generation pipeline; therefore, video coding related artifacts must first be mitigated to reliably revert stabilization transformations. Among such artifacts the most detrimental is caused by filtering of compressed video frames. Essentially, block-wise quantization of frame data during encoding introduces a blocking effect across block boundaries. To suppress these coding related visual artefact, H.264 and H.265 codecs incorporate filtering procedures both at the encoder and decoder. While this improves visual quality of resulting video significantly, it also weakens the inherent PRNU pattern. This weakening gets further emphasized at increasing compression levels. To address the disruptive effects of this filtering operation, [10] introduced a compensation method by modifying the decoder's operation. Results on test videos revealed that this method yields an improvement in measured PCE values with a three times average increase. Hence, we utilize this method to compensate for the effects of the filtering process when extracting video frames from the bitstream.

B. Frame-wise PRNU Extraction

Following the extraction of video frames, the process for inverting stabilization transformations starts. Since transformations are performed in the spatial domain, the search for the unknown transformation for each frame has to be ideally performed in the spatial domain where the correct transformation is validated based on the match of the estimated PRNU with the reference PRNU. That is, inverse transformation in spatial domain has to be followed by PRNU estimation. This order of operations, however, involves a significant amount of computation because transformation parameters are determined through a brute-force search and the search space for the parameters can be quite large. Due to this complexity, earlier work [12], [14], [15] changed the order of operations and searched for inverse transformation in the PRNU domain, rather than in the spatial domain, which is performed much

faster as PRNU estimation is performed only once. However, since the PRNU estimation operation is not of linear nature, this change in order is likely to introduce degradation in performance. Further, it must be noted that a geometric transformation also involves an interpolation operation as transformed coordinates will not correspond to grid positions in the original frame and missing values at those grid locations must be interpolated. Such interpolation will act as another disturbance on the underlying PRNU pattern.

To determine the overall impact of performing a search in PRNU domain on performance, we performed a test. For this purpose, we utilized videos taken under controlled conditions, by turning off stabilization and under low compression setting, using a custom camera application for Android mobile operating system [11]. The test included 1000 frames from videos taken by 6 cameras and the corresponding reference PRNU patterns. For each frame, we first evaluated the match with the reference PRNU pattern in terms of the PCE metric and determined that the average value for all frames is 219. To measure the impact of transformation related interpolation, we applied a random transformation and its inverse consecutively to each frame and computed the match of estimated PRNUs with reference patterns. Our evaluation of various widely used resampling methods, including the nearest neighbor, bicubic and bilinear interpolations, revealed that the nearest neighbor method induces the least distortion on the estimated PRNU pattern with the overall average dropping to 167. Finally, we applied the same sequence of random transformations to each frame, estimated PRNU patterns, inverted the transformation and re-evaluated the match with the reference PRNU which yielded the average of 162. The resulting PCE values show that search of parameters in the PRNU domain will potentially yield acceptable results in most cases.

To exploit the computational advantage, in our method, we also perform a search for inverse transform parameters in the PRNU domain. Hence, full-frame PRNU patterns are extracted individually from loop-filter compensated video frames using the basic method introduced in [1].

C. Stabilization Testing

The steps involved in the attribution of a stabilized video are computationally intensive. To effectively deal with this complexity, the level of stabilization applied to a video and how it is performed must also be taken into account. Therefore, rather than assuming that a video has undergone severe stabilization, it must first be checked for traces of weak stabilization by assuming an affine model for camera motion. Those videos can be attributed using earlier proposed approaches [12], [15], and only the remaining videos must be kept for further analysis considering more complex stabilization settings.

In line with this thinking, we perform two tests to eliminate unstabilized and weakly stabilized videos from further testing. To achieve this goal, we first apply a test, stb_{chk} , to verify the presence of a stabilization in a video. This is realized by estimating two reference patterns from the first and last third parts of a video by utilizing the basic method [1] on loop-filter compensated video frames and evaluating their match. Videos

determined to be stabilized are then subjected to another test, stb_{lite} , to identify weakly stabilized videos. This test is performed by geometrically aligning PRNU patterns of 10 I frames following the first I frame with respect to the reference pattern through a search of affine transformation parameters. Those frames that yield a PCE value of 38 after transform inversion are combined together to obtain a PRNU estimate as performed by [12]. If the resulting estimate yields a sufficient match, the test is considered a positive confirmation of weak stabilization. Videos that yield low values on both tests are kept for further analysis.

D. Frame Cropping

The most prominent stabilization approach involves application of spatially varying transformations to each frame rather than applying a global transformation. In its most simplest form, this reduces to splitting a frame into a grid and stabilizing each grid block locally where block sizes can be as small as 64×36 pixels [16] or 40×40 pixels [25]. With any stabilization approach, however, it is safe to assume that there will be some locality that has undergone a specific geometric transformation.

Therefore, the size of blocks that needs to be used during search for inverse transformation parameter must be determined. We performed tests to determine the smallest block size in a video frame that will yield meaningful PCE measurements. For this purpose we used seven unstabilized videos taken by different cameras with known reference PRNUs. The videos were compressed at the lowest possible compression and were captured indoors while the camera is moving [11]. In each frame, we cropped blocks of varying size, estimated the PRNU, and evaluated the match with the corresponding block in the reference PRNU. Figure 4 provides histograms of measured PCE values when block size is set to 50×50 , 100×100 , 250×250 ve 500×500 pixels. As it can be seen from these results PRNU blocks with sizes of 50×50 and 100×100 do not yield reliable measurements where most PCE values are much lower than the commonly accepted threshold value of 60. Even at the block size of 250×250 a significant number of blocks do not yield sufficiently high PCE values. Therefore, in our method, we utilize a block size of 500×500 but also incorporate results of 250×250 sub-blocks when identifying transformation parameters.

The other issue concerns the selection of the block location in each video frame. In our method, we select the 500×500 blocks at the center of each frame. This is primarily because of three reasons. First, the focal point is typically around the center of the frame, therefore stabilization related distortions are less likely to be in this region. Second, since edges of frames are likely to be created through an inpainting process following stabilization, this ensures exclusion of those parts of frames from estimation. And finally, by choosing the same location at each frame, corresponding PRNU extracts can be combined together to obtain a more reliable estimate.

E. Warping Inversion

Inversion of stabilization warps essentially corresponds to determining the correction applied to frames due to smoothing

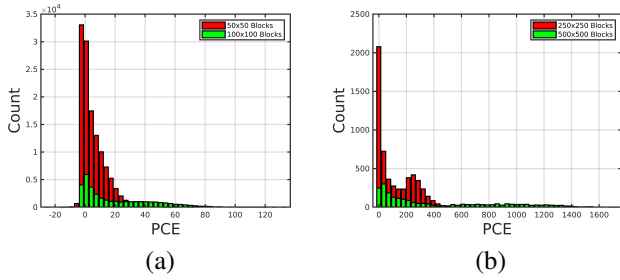


Fig. 4. Histogram of PCE measurements obtained by matching (a) 50×50 and 100×100 (b) 250×250 and 500×500 sized blocks to corresponding blocks in the reference PRNU pattern.

of estimated camera motion. In the absence of an unstabilized, original video, this can only be realized by performing a blind search for corresponding transformation parameters at a given locality. Obviously, the complexity of this task is determined by the nature of camera motion. At the simplest, an affine motion model can be assumed. This will be effective when camera motion is only limited to translations and rotations. However, since an affine transformation preserves the parallelism of lines (but not their lengths and angles), it cannot correct perspective projections introduced by a moving camera. Hence, to take into account more complex stabilization transformations, projective transformations can be utilized.

A projective transformation can be represented by a 3×3 matrix with 8 free parameters that specify the amount of rotation, scaling, translation, and projection applied to a point in two-dimensional space. In this sense, affine transformations form a subset of all such transformations without the two-parameter projection vector. Since a transformation is performed by multiplying the coordinate vector of a point with the transformation matrix; its inversion requires determining all these parameters. This problem is further exacerbated when transformations are applied in a spatially variant manner as different parts of the block might have undergone different transformations and when the block size is relatively small which yields to lower PCE values.

To determine the correct transformation applied to a block within a video frame, the block is inverse transformed repetitively and the transformation that yields the highest PCE between the inverse transformed block and the reference PRNU pattern is identified. In realizing this, rather than changing transformation parameters blindly which may lead to unlikely transformations and necessitate interpolation to take non-integer coordinates to integer values, we considered transformations that move corners of the block within a search window. In this regard, a large search window is preferable for more correct identification of the transform; however, search complexity grows polynomially with the size of the window.

In determining a window size, we utilized several videos manually stabilized using the iMovie video editing program. We observed that at 10% stabilization setting, KLT points move at most within a window of 15×15 pixels. In fact, this observation aligns well with findings of earlier work in the field. In [23], Liu *et al.* determined that considering dynamic scenes, points on tracked feature trajectories exhibit on average

an unwanted motion of 2.36 pixels with great majority of points moving less than 8.4 pixels overall. Obviously, with increasing camera motion such deviations are likely to increase. In [21], it is exhibited that low-frequency, up and down motions caused by walking may go up to 30 pixels. Similarly, Iuliani *et al.*, by providing measurements obtained from several videos (see variation in central cropping positions given in Table 3 of [12]), demonstrate that stabilization induced pixel movements can be within a range of ± 24 pixels.

Therefore, a larger search window is expected to increase the chances of determining the correct stabilization transformation at the expense of considerably more computation. In line with these observations, in our method, we assume that coordinates of each corner of a selected block may move independently within a window of 15×15 pixels, *i.e.*, spanning a range of ± 7 pixels in both coordinates with respect to original position. However, the block might have been subjected to a global translation (*e.g.*, introduced by a cropping) not contained within the searched space of transformations. To be able to detect such translations as well, each inverse transformed block is also searched within a shift range of ± 50 pixels in all directions in the reference pattern.

Further, to accelerate the search, instead of performing a pure random search over all coordinates, we adopted a three-level hierarchical grid search approach. Essentially, with this approach, the search space over rotation, scale, and projection is coarsely sampled. In the first level, each corner coordinate is moved by ± 4 pixels (in all directions) over a coarse grid to identify five transformations (out of 3^8 possibilities) that yield the highest PCE values. A higher-resolution search is then performed by the same process over neighboring areas of the identified transformations on a finer grid by changing the corner coordinates of transformed blocks ± 2 and, again, retaining only the 5 transformations producing the five highest values. Finally, in the third level, coarse transformations determined in the previous level are further refined by considering all neighboring pixel coordinates (around a ± 1 range) to identify the most likely transformations needed for inverting the warping transformation due to stabilization. This overall reduces transform search space from 15^8 to 11×3^8 possibilities, thereby yielding a significant reduction in complexity. A pictorial depiction of the grid partitioning of the transform space is shown in Fig. 5.

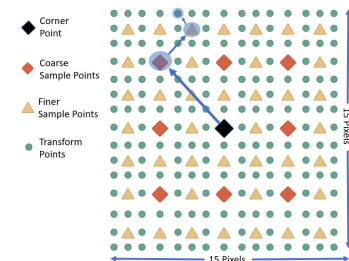


Fig. 5. Three-level hierarchical grid partitioning of transform space. Coarse grid points that yield high PCE values are more finely partitioned for subsequent search. The arrows shows a sample trace of search steps to identify a likely transformation point for one of the corner points of a selected block.

F. Transform Validation

Due to various factors, such as spatially variant nature of stabilization, coarse sampling of transformation space, small block size, and further weakening of PRNU patterns in video frames by compression and downsizing, very high PCE values may not be achieved even after correctly inverting the transformation. (It must be noted that the reliability of a PRNU pattern extracted from a video frame that underwent compression using the typical quantization parameter value of 20 is comparable to JPEG compression at quality factor of 65 [10].) Therefore, the warping inversion step might return an incorrect transformation due to a spurious match. To assess the correctness of the identified inverse transformation, this step incorporates following additional measures.

- PCE_{vld} : A validation threshold is set to eliminate an unlikely transformation associated with a selected block. When warping inversion yields a PCE value lower than PCE_{vld} , the identified transformation is assumed to be incorrect, and those blocks are excluded from PRNU estimation. To prevent false eliminations, this threshold must be set to a value well below the commonly accepted decision threshold used for photos, *i.e.*, PCE value of 60.
- (n_{sub}, PCE_{sub}) : It is likely the inverse transformed PRNU block involves parts of frame content that underwent different warpings during stabilization. To ensure that the identified transformation is largely prevalent over the block and is not due to some localized, content interference related phenomena, we test whether the four non-overlapping 250×250 blocks comprising the central 500×500 block exhibit some coherence in the matching behavior. To realize this, the number of inverse transformed sub-blocks that yield a PCE value above a specified threshold (PCE_{sub}) are determined. If this number is above a predetermined value (n_{sub}) the block is assumed to be correctly inverse transformed.

When the PCE values associated with a block and its sub-blocks are found to be below threshold values, *i.e.*, PCE_{vld} and PCE_{sub} , a PRNU pattern could not be estimated from that particular frame. In that case, warping inversion and transform validation steps are applied to remaining video frames. It must be noted that, if none of the frames yield a PRNU pattern (regardless of whether sources match or not) the source of the video in question is considered to be not verified.

G. Weighting & PRNU Pattern Estimation

In the last step, remaining PRNU patterns corresponding to central 500×500 block in each frame, following warping inversion and validation steps, are combined together to obtain a more reliable estimate of the sensor's PRNU. With videos, the reliability of the extracted PRNU pattern depends also on the level of compression applied during video coding. Since encoder operates at a macroblock level by quantizing blocks at varying strengths, each macroblock's PRNU contribution can be weighted to take into account quantization related information loss to obtain a better estimate. Hence, an estimate pattern is obtained by simply taking an average of weighted PRNU patterns using the weighting scheme described in

[10]. This is essentially realized by creating a frame-level-mask with weighting coefficients determined based on the size, location, and quantization parameter of each macroblock. (An implementation for the PRNU weighting scheme can be obtained at the link in the footnote of second page.) It must be noted that the mask corresponding to each frame is also transformed by the same transformation identified for a block. The overall estimate obtained through PRNU weighting is then matched with the camera's reference PRNU to finally make an attribution decision.

V. PERFORMANCE EVALUATION

To test the effectiveness of our method we used a standard dataset and two custom-built datasets.

A. Datasets

1) *VISION dataset*: This dataset includes a collection of photos and videos captured by 35 different camera models [33]. The videos in the dataset are divided into three sub-categories in terms of their content characteristics as having flat background, indoor, and outdoor scenes. For each content sub-category three types of videos are acquired under increasing camera motion where the camera was still, moving, and manually panned and rotated. (These different types of videos will be shortly referred to as still, move, or panrot videos.) All videos are about 70 seconds long and initially acquired using the native camera application. Out of the 35 cameras, only 16 of them performed stabilization with 13-32 videos available per camera. This provided us with a total of 295 original videos captured by these cameras. Out of these videos, however, 38 of them had a low resolution (less than 1920×1080 pixels) and, therefore, were removed from further analysis.

To measure the source camera verification accuracy, all of the 257 full-HD, stabilized videos are used during tests. In all cases, the reference PRNU pattern for each camera is obtained using photos captured by the same camera. The amount of cropping and scaling applied to the full-frame sensor output to obtain video frames by in-camera downsizing are determined based on findings of [15], which reported both parameters for corresponding cameras in the VISION dataset. The tests are also repeated using non-matching reference PRNU patterns to measure the false-positive rate of the method.

Our method is devised to verify the source of stabilized videos where transformations are more complex than application of frame-level affine transformations. To identify those strongly stabilized videos, we set the thresholds for stb_{chk} and stb_{lite} tests to PCE values of 60 and 100, respectively. This resulted with elimination of the 105 out of the 257 tested videos by the stb_{chk} test as they can already be successfully attributed to their sources. The remaining 152 videos are then subjected to stb_{lite} test to identify weakly stabilized ones. This is realized by aligning PRNU patterns of I frames with respect to the reference pattern obtained from photos through a search of transformation parameters considering scaling factors around the values determined in [15] for all cameras, rotations up to $\pm 1.5^\circ$ with 0.1° increments, and all possible

shift positions, as performed by [12] while setting aggregation threshold to a PCE value of 38. Overall, 108 videos, out of 152, could be reliably attributed to their sources under a frame-level affine transformation model. Hence, this left us with 44 strongly stabilized videos that cannot be attributed using earlier proposed approaches. Examination of these videos revealed that, except for one, they belong to the panrot and move video categories where acquisition is performed under translational camera motion. An attempt to verify the source of these videos on a frame-by-frame basis using the basic method resulted with only two frames exceeding the PCE value of 60 (with values 78 and 491) while most frames yielded values less than 10. This further showed that stabilization transformations were applied to almost all frames.

2) *iPhone SE-XR Dataset*: This includes a collection of images and videos captured by two smartphone models, namely, iPhone Special Edition (SE) and iPhone XR. These two models are selected due to two main reasons. First, they are more recent smartphone models, and therefore, they plausibly deploy a state-of-the-art, in-camera stabilization solution. Second, both phone models feature only one main camera which prevents any potential post-processing related complications due to availability of multiple cameras (such as HDR/WDR processing, noise reduction, *etc.*). This dataset includes media captured by 8 different phones (2 iPhone SE and 6 iPhone XR models) with a total of 263 photos and 41 videos (11-54 photos and 2-14 videos per camera). These media are collected by searching for public Flickr profiles and using phones that we had access to. Sources of Flickr photos are validated through pair-wise matching ($PCE > 60$) and through metadata verification. Another criterion we used for inclusion in the dataset was the availability of at least one still or low-motion video to ensure success of source verification and parameter estimation.

Following frame extraction with compensation for loop filtering and frame level PRNU pattern estimation, the two stabilization tests conducted. Firstly, through the stb_{chk} test it is determined that all videos are indeed stabilized. Then the reference PRNU patterns needed for source verification are obtained from photos; however unlike in the case of VISION dataset, the scaling factor used for downsizing photos to frames were not known a priori and had to be determined. For this purpose, the photo-based PRNU reference pattern and the PRNU pattern from the first frame of videos are matched considering rotations up to $\pm 1.5^\circ$ with 0.1° increments, all shift positions, and all scaling factors in the range of 0.3 to 0.9 with increments of 0.01. The search for involved parameters revealed that iPhone XR and SE perform scaling with factors around 0.86 and 0.79, respectively. The stb_{lite} test is then conducted as done for the VISION dataset using identified scaling factors for every video with 10 successive I frames following the first I frame. (For videos with less than 11 I frames, maximum number of available I frames are used.) In cases where a match could not be attained, scaling factors obtained for other videos of the same camera model are also tried with the video in test. Overall, following the stb_{lite} test, source of 19 videos could be verified and 22 videos

whose source could not be verified are identified as strongly stabilized.

3) *Adobe Premiere Pro Stabilized (APS) Video Dataset*: This dataset includes videos captured by 7 Android OS based smartphones through a custom camera application that turns off electronic stabilization and digital zoom and uses the camera’s default compression setting [11]. It contains a total of 30 videos with 4-5 videos per camera. Videos are shot indoors under a smooth panning motion with durations varying from 4-6 seconds. (The list of camera models and the number of available videos captured by each camera are given in Appendix A.) One of the videos from each camera is used to obtain a reference PRNU pattern while the remaining 23 videos are externally stabilized using Adobe Premiere Pro software suite. The choice of this software is due to its explicit indication of performing spatially variant stabilization [34]. Videos are stabilized at 10% stabilization level while allowing frame-cropping but without post-stabilization scaling. For these cameras, since the reference PRNU pattern can be obtained from a non-stabilized video, determining a scaling factor was not a concern. Therefore, when performing the stb_{lite} test only a slight scaling (with factors of 1 ± 0.01), rotations in the above specified range, and shifts within a range of ± 100 pixels are considered as parameters of affine transformations. It is verified through this test that out of the 23 videos 8 are weakly stabilized and 15 are strongly stabilized.

Table I provides a brief description of the three video datasets in terms of their stabilization characteristics.

TABLE I
DATASET FEATURES

Dataset	# of Cameras	# of unstabilized videos	# of weakly stabilized videos	# of strongly stabilized videos
VISION	14	105	108	44
iPhone SE-XR	8	0	19	22
APS	7	0	8	15

B. Results

Before performing attribution tests, a number of parameters related to our proposed approach must be determined. Most notably, this concerns the transform validation step which is necessary for eliminating transformations that are very likely to be incorrect. To accept or reject an identified transformation associated with a block, resulting PCE value is first compared to the PCE_{vld} . Then, a validation is performed at the sub-block level which includes an acceptance threshold for each sub-block and the minimum number of blocks that need to exceed this threshold, *i.e.*, (n_{sub}, PCE_{sub}) .

To determine these three parameters for each dataset, we utilized 5 frames from each of the strongly stabilized videos. Using the camera reference patterns and a set of arbitrary non-matching patterns, we performed transform inversion on central 500×500 blocks of all frames to identify the transformations that yield the best match. We then performed a sweep over the three parameters considering the whole

range of values 0 – 40 for PCE_{vld} , 0 – 4 for n_{sub} , and 0 – 5 for PCE_{sub} that maximises correct identification rate while false identification among non-matching cases is set to zero. Based on the observed accuracy values, best results are achieved when validation parameters are set to $PCE_{vld} = 28$, $n_{sub} = 2$, and $PCE_{sub} = 2$ for all datasets except for the APS dataset for which n_{sub} is found to be 1. Overall, despite a slight variation, this finding shows that the determined parameter values generalize well over the three datasets. To further verify that this is indeed the case, we repeated the same process by combining the 81 strongly stabilized videos from all datasets together and determining overall parameters jointly. This yielded $PCE_{vld} = 28$, $n_{sub} = 2$, and $PCE_{sub} = 2$, as expected.

An important concern with attribution of stabilized videos is a misidentification of warping transformations due to typically low PCE values. To contain such occurrences, we keep track of top five transformations that yield highest PCE values rather than only retaining the best one. Hence, when evaluating the accuracy of the method, we consider the correct transformation to be among these transformations. In accordance with this, in the last step, five PRNU estimates are obtained rather than just one. The first estimate is obtained using the best of the top-five transformations for each frame, the second using the second best of top-five, and so on. Then, each resulting estimate is matched with the reference PRNU pattern. Since identified transformations are expected to converge, an attribution decision is made only if three of the top-five identified transformations yield a PCE value above the designated threshold.

When verifying the source of a video, we utilized a number of frames from each given video. Although attribution accuracy will improve with the number of frames, the computational complexity forbids using a large number of frames. For this purpose, we only utilized I frames which are used for prediction of other frames and, therefore, undergo a more favorable compression during coding. Further, leaving a temporal gap between frames makes warping inversion step less affected by video content and thereby less prone to errors. For our tests, we used 5 and 10 successive I frames from each video to evaluate the method’s performance. In all videos, first I frames are excluded from attribution as some cameras either do not stabilize the first frame or perform a lighter stabilization than the subsequent frames. When determining the correct attribution rate, each strongly stabilized video in the three datasets are matched with the reference pattern of corresponding camera using parameters determined for each dataset (*i.e.*, PCE_{vld} , n_{sub} , PCE_{sub}). To also measure the false attribution rate, these tests are then repeated on a collection of 189 videos, including all stabilized videos in the VISION dataset (152) and all strongly stabilized videos in the APS and iPhone SE-XR datasets (37), using the parameters associated with each dataset and by matching each video with a randomly selected, non-matching reference PRNU pattern.

Figure 6 provides ROC curves showing the relation between true and false positive rates (TPR and FPR) at varying decision thresholds for the three datasets obtained using different number of frames. It must be noted that some of the videos in the

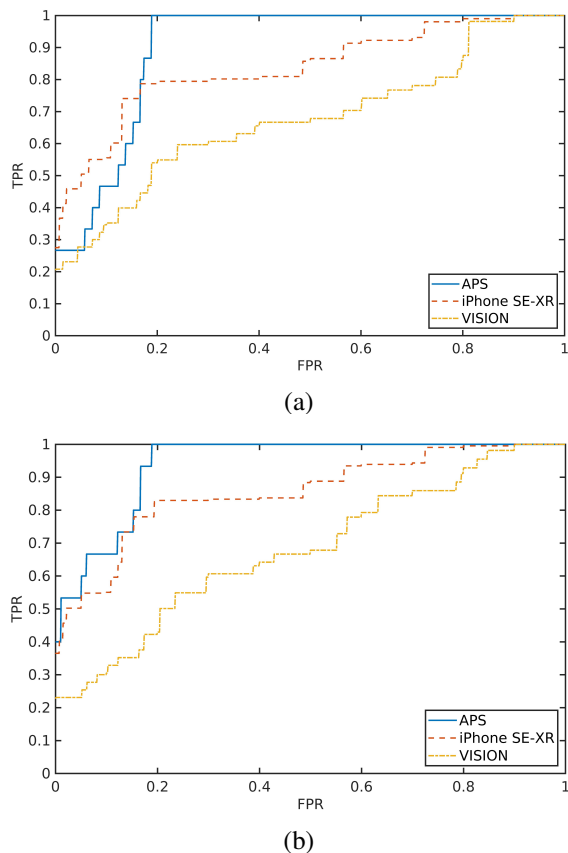


Fig. 6. True and false positive attribution rates obtained for the 3 datasets when using (a) 5 and (b) 10 successive I frames from each video. Each pair of ROC curves is obtained using 15, 19, and 44 strongly stabilized videos in each dataset with matching sources and 189 stabilized videos with randomly selected, non-matching sources.

APS and iPhone SE-XR datasets do not have 10 I frames. For those videos results are obtained using all available I frames along with some randomly selected frames to reach 10 frames. From the ROC curves it is determined that when only 5 frames are used for attributing videos in the APS, iPhone SE-XR, and VISION datasets, that cannot be attributed otherwise, our method, respectively, achieves a TPR of 27%, 27%, and 20% if FPR is set to 0%. Increasing the number of frames from 5 to 10 further improves the TPR in attribution of strongly stabilized videos to 40%, 36%, and 23%, respectively, at 0% FPR.

When evaluated together, these results show that, depending on whether 5 or 10 frames are used for attribution, proposed method is able to correctly attribute 19 to 24 of the 81 strongly stabilized videos in the three datasets, yielding a TPR of 23.4% to 29.6% at 0% FPR. Alternatively, instead of using parameters (*i.e.* PCE_{vld} , n_{sub} , PCE_{sub}) determined separately for each dataset, when jointly determined parameters for the combined dataset is used, all but two of the those videos can be correctly attributed at 0% FPR. Both of these videos are determined to be from the APS dataset. Overall, these results show that our method improves the state-of-the-art in attribution of strongly stabilized videos significantly.

We also determined the overall achievable attribution accu-

racy on these datasets. Considering the 152 stabilized videos in the VISION dataset, incorporation of our end-to-end approach (see Fig. 3) with existing methods focusing on attribution of weakly stabilized videos improves achievable attribution rate from 71% to 77% when using 5 frames and to 77.6% when using 10 frames, at 0% FPR in both cases. (It must be noted here that earlier work, [12] and [15] which mainly assume a frame-level affine transform model, reported results on VISION dataset considering videos captured by all cameras that support stabilization in their tests. Hence, the disparity between their results and the 71% figure stems from the fact that our labeling of a video in the VISION dataset as stabilized or non-stabilized is mainly determined by stb_{chk} test rather than inferring the label based on ability of the capturing camera to perform stabilization.) Similarly for the iPhone SE-XR dataset overall attribution performance improved from 46% to 61% when using 5 frames and to 66% when using 10 frames for attribution. Finally, on the APS dataset overall accuracy increased from 35% to 52% with 5 frames and to 61% with 10 frames.

We further evaluated how utilizing individual transformations among identified top-five transformations affects performance in making an attribution decision. Figure 7 shows TPR and FPR curves obtained for varying PCE threshold values using 5 I frames from 81 strongly stabilized videos and 189 non-matching videos where in each case only one of the top-five (inverse) transformations is used for attribution. It can be seen from these results that all transformations yields similar results. This result verifies that warping inversion does not identify arbitrary transformations and that it converges towards a very closely related set of transformations. Therefore, the performance does not depend on which of the top-five transformations are used for making a decision.

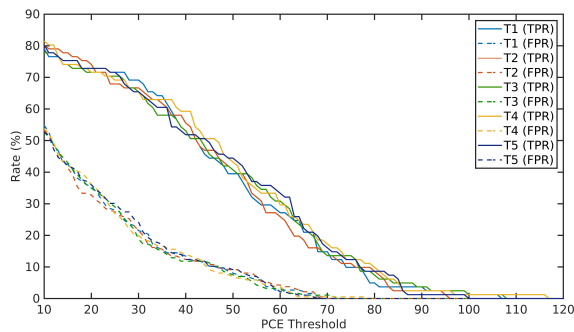


Fig. 7. Change in attribution rates when top five identified transformations (T_1, \dots, T_5) are used individually to make a decision. Curves are obtained under the same test setting as in Fig. 6 while utilizing only 5 frames from each video.

An important component of our method is the transform validation step mainly introduced to eliminate incorrectly identified transformations. Hence, this step is expected to be more effective in preventing false positive attributions. However, since the PRNU block size of 500×500 is large enough to potentially include content that has undergone different transformations during stabilization, it will also eliminate some of the true positive matches. To evaluate the impact of

transform validation step on videos with matching and non-matching cases, we examined the number of frames eliminated by it. Considering the earlier specified joint parameter values of $PCE_{vld} = 28$, $n_{sub} = 2$ and $PCE_{sub} = 2$ and the 81 videos with matching sources, we determined that this step eliminated 1.69 frames on average when 5 frames are used for attribution. Similarly, for the 189 videos with mis-matching sources, the average number of eliminated frames is found to be 3.5. In contrast, when 10 frames are used for attribution, on average 3.76 and 6.48 frames are eliminated for the source matching and non-matching cases, respectively. This result reveals that transform validation step essentially eliminates many more frames of videos with mis-matching sources as compared to matching sources. As a consequence, this allows PRNU patterns extracted from various frames of a video to be combined together to obtain a more reliable PRNU estimate, which in turns yields a higher overall PCE value for correct attributions.

To complement this, we next tested the importance of the transformation validation step on the correct attribution performance. For this, we first selectively removed the block ($PCE_{vld} = -\infty$) and sub-block ($n_{sub} = 0, PCE_{sub} = -\infty$) level measures utilized by the validation step before eliminating it completely. In each case, the remaining measure is selected to achieve zero false attributions while maximizing correct attributions. Table II provides the number of correctly attributed videos for the three cases. It can be seen from these results that just validating based on the PCE_{vld} value is more effective than imposing (n_{sub}, PCE_{sub}) values as it results with attribution of 12 videos as opposed to 6 videos attributed by using only the latter measure. If the transform validation step is removed completely, however, the number of attributed videos further drop to 5 videos from the initially attributed 19 videos. These results underline the key role of transform validation step in elimination of non-matching videos.

TABLE II
NUMBER OF CORRECTLY ATTRIBUTED VIDEOS WITH AND WITHOUT TRANSFORM VALIDATION STEP USING 5 FRAMES

Method	APS	iPhoneSE-XR	VISION
With Validation	4	6	9
$PCE_{vld} = -\infty$	1	2	3
$(n_{sub} = 0, PCE_{sub} = -\infty)$	2	3	7
Without Validation	1	1	3

To ensure that extracted PRNU patterns from the remaining frames contribute towards a more reliable PRNU estimate, we computed both the average PCE values corresponding to each block and the estimate reference pattern obtained by combining these individual PRNU patterns. For this, we examined all videos that have more than one frame that passed the transform validation step, regardless of whether the video is correctly stabilized or not. When the sources matched (*i.e.*, for the 81 videos), we determined that the PCE values corresponding to inverse transformed blocks increases on average from 33 to 48 when combined together. In the case of successfully attributed videos, the average PCE value increases from 37.8 to 77.8 after combining PRNU patterns. In the non-matching case, considering the 189 videos that yielded

more than one transform validated frames, we determined that PCE decreases from 25 to 18. These results overall show that our method can obtain an estimate of the PRNU pattern under more complicated stabilization settings.

C. Time Complexity

Overall, the computational complexity of the proposed approach is mainly determined by the number of transformations performed during the warping inversion step. In this regard, the described three-level hierarchical grid partitioning based search involved application of 72, 171 inverse transformations to a 500×500 sized PRNU noise block extracted from each frame. Tests were performed on a workstation with Intel Core i7-7700k CPU, 4.20 GHz, 32 GB RAM, running Ubuntu 18.04.1 LTS operating system. Our non-optimized end-to-end implementation of the verification method, based on sequential search of transform space, took on average 35 minutes to process each frame.

VI. DISCUSSION AND CONCLUSIONS

State-of-the-art stabilization methods pose a major challenge to source attribution of videos. The difficulty mostly stems from the spatially variant nature of stabilization transformations which is further exacerbated by the adverse effects of in-camera processing steps, such as downsizing and video compression. Essentially, addressing this requires blindly inverting a geometric transformation while at the same time being restricted to operate on smaller blocks with significantly weakened PRNU patterns. Our findings in this work show that under strong stabilization, reliable estimation of a PRNU pattern from a video is not viable. Instead, the problem can be addressed in a source verification setting, where the match of a video with a known camera is in question.

There is little information on details of stabilization methods deployed by cameras; therefore, it is not trivial to design methods that can provide optimal solutions with low computational cost. Although estimation of PRNU patterns through inversion of frame-level affine transformations constitute the first step of a solution for attribution, as demonstrated by our results, this approach is not adequately effective on all stabilized videos in the VISION and iPhone SE-XR datasets. To address this gap, our approach in this work builds on existing work in the field and expands capabilities to address more complicated forms of stabilization by assuming more degrees of freedom in the involved transformations and taking into account spatially variant nature of modern stabilization approaches. Results obtained on strongly stabilized videos in the VISION, iPhone SE-XR, and APS datasets show that our method, respectively, achieves a source verification accuracy of 20-23%, 27-36%, and 27-40% when using 5-10 frames for attribution.

The novelty of our method mainly stems from tackling the spatially variant nature of stabilization methods by searching a large range of projective transformations at sub-frame level and due to its ability to eliminate incorrectly identified transformations. Although our method improves existing capabilities considerably, reliable attribution of strongly stabilized

videos requires further exploration. One potential improvement area concerns obtaining further specifics about the stabilization methods deployed by cameras in smartphone type computing devices. Such an information can be translated into devising more effective warping inversion methods. Another advancement that will help achieve better results is about reliable estimation of PRNU patterns. Since with video frames smaller block sizes yield very weak PRNU patterns, overcoming this obstacle will have a direct impact on the success of warping inversion step. Recently proposed deep learning based approaches [35] can be considered a step in this direction.

Finally, we note that since transform inversion is done in a blind manner, incorrect identification of transformations is more likely to occur with increasing search space. Therefore, transform validation step is of vital importance to our method. Initially, when determining transformation parameters, we also considered imposing a continuity constraint between transformations applied to successive frames as the camera motion cannot change abruptly from one frame to another. Our analysis, however, revealed that even videos with non-matching sources exhibit this characteristic. That is, PRNU patterns extracted from two successive frames under very similar transformations may also yield similar PCE values with a non-matching reference PRNU pattern. We conjecture that this behavior is mainly due to the content interference in the estimated PRNU pattern of successive frames. Hence, it is necessary to sample frames from different parts of a video to suppress content dependency effects.

VII. ACKNOWLEDGEMENT

This work is supported by the Scientific and Technological Research Council of Turkey (TUBITAK) grant 116E273. We also thank E. S. Tandogan for his help in conducting some of the experiments.

APPENDIX

The camera models used for capturing videos in the APS dataset under controlled settings [11] (*i.e.* with stabilization and electronic zoom turned off and at default video compression settings) are listed below. The numbers in parentheses denote the number of videos available from each camera.

Samsung Edge 6 (5)	Redmi 5 Plus (5)	LG G4 (4)	Galaxy S4 (4)
Huawei P20 Lite (4)	LG G Flex2 (4)	LG G3 (4)	

REFERENCES

- [1] M. Chen, J. Fridrich, M. Goljan, and J. Lukás, "Determining image origin and integrity using sensor noise," *IEEE Transactions on information forensics and security*, vol. 3, no. 1, pp. 74–90, 2008.
- [2] B. V. K. V. Kumar and L. Hasebrook, "Performance measures for correlation filters," *Appl. Opt.*, vol. 29, no. 20, pp. 2997–3006, Jul 1990. [Online]. Available: <http://ao.osa.org/abstract.cfm?URI=ao-29-20-2997>
- [3] P. Corcoran, P. Bigioi, J. Chen, W. Cranton, and M. Fihn, "Consumer imaging i-processing pipeline, focus and exposure," pp. 1–25, 2016.
- [4] J. Zhang, J. Jia, A. Sheng, and K. Hirakawa, "Pixel binning for high dynamic range color image sensor using square sampling lattice," *IEEE Transactions on Image Processing*, vol. 27, no. 5, pp. 2229–2241, 2018.
- [5] J. Guo, H. Gu, and M. Potkonjak, "Efficient image sensor subsampling for dnn-based image classification," in *Proceedings of the International Symposium on Low Power Electronics and Design*, 2018, pp. 1–6.

- [6] M. Chen, J. Fridrich, M. Goljan, and J. Lukáš, "Source digital camcorder identification using sensor photo response non-uniformity," in *Security, Steganography, and Watermarking of Multimedia Contents IX*, vol. 6505. International Society for Optics and Photonics, 2007, p. 65051G.
- [7] D.-K. Hyun, C.-H. Choi, and H.-K. Lee, "Camcorder identification for heavily compressed low resolution videos," in *Computer Science and Convergence*. Springer, 2012, pp. 695–701.
- [8] W.-H. Chuang, H. Su, and M. Wu, "Exploring compression effects for improved source camera identification using strongly compressed video," in *Image Processing (ICIP), 2011 18th IEEE International Conference on*. IEEE, 2011, pp. 1953–1956.
- [9] E. Altınışık, K. Tasdemir, and H. T. Sencar, "Extracting prnu noise from h.264 coded videos," in *2018 26th European Signal Processing Conference (EUSIPCO)*. IEEE, 2018, pp. 1367–1371.
- [10] E. Altınışık, K. Taşdemir, and H. T. Sencar, "Mitigation of h.264 and h.265 video compression for reliable prnu estimation," *IEEE Transactions on information forensics and security*, 2019.
- [11] E. S. Tandogan, E. Altınışık, S. Sarimurat, and H. T. Sencar, "Tackling in-camera downsizing for reliable camera id verification," in *Electronic Imaging, Media Watermarking, Security, and Forensics*. Society for Imaging Science and Technology, 2019.
- [12] M. Iuliani, M. Fontani, D. Shullani, and A. Piva, "Hybrid reference-based video source identification," *Sensors*, vol. 19, no. 3, p. 649, 2019.
- [13] S. Taspinar, M. Mohanty, and N. Memon, "Source camera attribution of multi-format devices," *arXiv preprint arXiv:1904.01533*, 2019.
- [14] —, "Source camera attribution using stabilized video," in *2016 IEEE International Workshop on Information Forensics and Security (WIFS)*. IEEE, 2016, pp. 1–6.
- [15] S. Mandelli, P. Bestagini, L. Verdoliva, and S. Tubaro, "Facing device attribution problem for stabilized video sequences," *IEEE Transactions on Information Forensics and Security*, 2019.
- [16] F. Liu, M. Gleicher, H. Jin, and A. Agarwala, "Content-preserving warps for 3d video stabilization," in *ACM Transactions on Graphics (TOG)*, vol. 28, no. 3. ACM, 2009, p. 44.
- [17] D. Shullani, M. Fontani, M. Iuliani, O. Al Shaya, and A. Piva, "Vision: a video and image dataset for source identification," *EURASIP Journal on Information Security*, vol. 2017, no. 1, p. 15, 2017.
- [18] "Developer.apple.com," 2020, January. [Online]. Available: <https://developer.apple.com/library/archive/documentation/DeviceInformation/Reference/iOSDeviceCompatibility/Cameras/Cameras.html#>
- [19] B. Golik and D. Wueller, "Measurement method for image stabilizing systems," in *Digital Photography III*, vol. 6502. International Society for Optics and Photonics, 2007, p. 65020O.
- [20] J. Xu, H.-w. Chang, S. Yang, and M. Wang, "Fast feature-based video stabilization without accumulative global motion estimation," *IEEE Transactions on Consumer Electronics*, vol. 58, no. 3, pp. 993–999, 2012.
- [21] M. Grundmann, V. Kwatra, and I. Essa, "Auto-directed video stabilization with robust 11 optimal camera paths," in *Proceedings of CVPR 2011*. IEEE, 2011, pp. 225–232.
- [22] D. J. Thivent, G. E. Williams, J. Zhou, R. L. Baer, R. Toft, and S. X. Beysserie, "Combined optical and electronic image stabilization," May 22 2018, uS Patent 9,979,889.
- [23] S. Liu, L. Yuan, P. Tan, and J. Sun, "Steadyflow: Spatially smooth optical flow for video stabilization," in *Proceedings of the IEEE Conference on Computer Vision and Pattern Recognition*, 2014, pp. 4209–4216.
- [24] J. Kopf, "360 video stabilization," *ACM Transactions on Graphics (TOG)*, vol. 35, no. 6, p. 195, 2016.
- [25] Z. Wang, L. Zhang, and H. Huang, "High-quality real-time video stabilization using trajectory smoothing and mesh-based warping," *IEEE Access*, vol. 6, pp. 25 157–25 166, 2018.
- [26] B. D. Lucas and T. Kanade, "An iterative image registration technique with an application to stereo vision," 1981.
- [27] C. Tomasi and T. K. Detection, "Tracking of point features," Tech. Rep. CMU-CS-91-132, Carnegie Mellon University, Tech. Rep., 1991.
- [28] M. Goljan and J. Fridrich, "Camera identification from cropped and scaled images," in *Security, Forensics, Steganography, and Watermarking of Multimedia Contents X*, vol. 6819. International Society for Optics and Photonics, 2008, p. 68190E.
- [29] A. Karaküçük, A. E. Dirik, H. T. Sencar, and N. D. Memon, "Recent advances in counter prnu based source attribution and beyond," in *Media Watermarking, Security, and Forensics 2015*, vol. 9409. International Society for Optics and Photonics, 2015, p. 94090N.
- [30] L. Bondi, P. Bestagini, F. Perez-Gonzalez, and S. Tubaro, "Improving prnu compression through preprocessing, quantization, and coding," *IEEE Transactions on Information Forensics and Security*, vol. 14, no. 3, pp. 608–620, 2018.
- [31] M. Goljan, "Blind detection of image rotation and angle estimation," *Electronic Imaging*, vol. 2018, no. 7, pp. 1–10, 2018.
- [32] M. Grundmann, V. Kwatra, and I. Essa, "Cascaded camera motion estimation, rolling shutter detection, and camera shake detection for video stabilization," Feb. 6 2018, uS Patent 9,888,180.
- [33] D. Shullani, M. Fontani, M. Iuliani, O. Al Shaya, and A. Piva, "Vision: a video and image dataset for source identification," *EURASIP Journal on Information Security*, vol. 2017, no. 1, p. 15, 2017.
- [34] "Adobe premiere," 2020, January. [Online]. Available: <https://www.adobe.com/products/premiere.html>
- [35] M. Kirchner and C. Johnson, "Spn-cnn: Boosting sensor-based source camera attribution with deep learning," in *2019 IEEE International Workshop on Information Forensics and Security (WIFS)*. IEEE, 2019.